Raman scattering of indium-rich $Al_xIn_{1-x}N$: Unexpected two-mode behavior of $A_1(LO)$

Ting-Ting Kang (康亭亭),* Akihiro Hashimoto（橋本明弘), and Akio Yamamoto（山本暠勇)
Department of Electrical and Electronics Engineering, Graduate School of Engineering, University of Fukui, Bunkyo 3-9-1, Fukui 910-8507, Japan

(Received 19 August 2008; revised manuscript received 5 November 2008; published 7 January 2009)

$Al_xIn_{1-x}N$ films ($0.03 \leq x \leq 0.80$), particularly indium-rich AlInN films, are studied by Raman scattering. We clearly observe a two-mode behavior of $A_1(LO)$ phonon and prove that the previous theoretical prediction and experimental attribution of InN-like $A_1(LO)$ to E_2^H mode are incorrect. Using the modified random-element isodisplacement model of Chang and Mitra, the information about AlInN lattice vibration is extracted. We believe that these results imply a strong positive force interaction between In and Al sublattices in AlInN. The strong interaction makes AlInN different with AlGaN in $A_1(LO)$ phonon mode behavior.

DOI: 10.1103/PhysRevB.79.033301 PACS number(s): 78.30.Ly, 71.55.Eq, 63.20.−e

The lattice dynamics of random alloys is a complex issue. The complexity results from the interplay of different lattice bonds due to composition variation. An important phenomenon in this field is the mode behavior of long-wavelength optical phonons. It is known that ternary mixed crystals $A_xB_{1-x}C$ with fully pronounced random alloy character are classified into two main classes according to the behavior of zone-center optical phonons. In the one-mode class, the frequencies vary continuously and approximately linearly with the molar fraction x of the alloy. In the case of two-mode behavior, there are two sets of optical modes corresponding nearly to those of two pure crystals AC or BC which compose the alloy. These extra modes may persist very close to the end compositions, i.e., $x=0$ and $x=1$.[1]

In order to determine the mode behavior of long-wavelength optical phonons in mixed crystals, using the modified random-element isodisplacement (MREI) model, Chang and Mitra[2] deduced their criteria in 1968. These criteria are for $A_xB_{1-x}C$, m_A, m_B, m_C are the atomic masses of atoms A, B, and C, and $m_A < m_B$. If $m_A < \mu_{BC}$ [$\mu_{BC} = m_B m_C/(m_B+m_C)$ is the reduced mass of atoms B and C], it exhibits two-mode behavior; whereas the opposite is true for the one-mode behavior. These criteria succeed in interpreting many experimental results, such as the two-mode behavior for longitudinal optical (LO) phonons in AlGaAs (Ref. 3) and AlInAs (Ref. 4) and the one-mode behavior for $A_1(LO)$ in hexagonal MgZnO.[5]

For III-nitride alloys, the most extensively studied one is AlGaN. Raman scattering has shown that E_2^H phonon shows two-mode behavior and $A_1(LO)$ shows one-mode behavior.[6] The one-mode behavior for longitudinal phonons $A_1(LO)$ is in good agreement with the one-mode criteria of Chang and Mitra,[2] i.e., $m_{Al} > \mu_{GaN}$, because of the much smaller mass of nitrogen atom than Al and Ga atom. Those observations have stimulated a lot of theoretical research to interpret the experimental results of AlGaN and predict the future results of other III-nitride alloy, including AlInN, for which one-mode criteria $m_{Al} > \mu_{InN}$ are still satisfied well. They have usually adopted various versions of MREI model as theoretical basis.[7,8] For example, Grille *et al.*[7] predicted that for AlInN, $A_1(LO)$ also exhibits one-mode behavior and E_2^H exhibits two-mode behavior.

Naik *et al.*[9] used Raman scattering to study the mode evolution of their $Al_xIn_{1-x}N$ samples grown by molecular-beam epitaxy (MBE) with $0.3 \leq x \leq 1$. Guided by the theoretical results of Grille *et al.*,[7] Naik *et al.*[9] concluded that $A_1(LO)$ shows one-mode behavior and attributed the two modes below $A_1(LO)$ in their Raman spectra to AlN-like and InN-like E_2^H modes. However, they had noticed the abnormally large splitting of two "E_2^H" modes in Al-rich samples.

The convincible knowledge about AlInN phonon requires a careful study of AlInN over the whole composition range. Nevertheless, the expected large immiscibility of AlInN alloy makes the material preparation a great challenge, especially for indium-rich AlInN. Recently, attracted by AlInN 0.7–6.2 eV wide band-gap energy coverage and the resulting potential applications, we have developed an AlN buffer technology to grow high-quality indium-rich AlInN by metal-organic chemical vapor deposition (MOCVD). Using this technology, we can grow $Al_{0.2}In_{0.8}N$ with full width at half maximum (FWHM) in $(0002)\theta/2\theta$ scan (ω scan) being 595 arc sec (2276 arc sec), which is much better than the reported MOCVD AlInN films,[10,11] and even some better than MBE-grown AlInN reported by Chiba university.[12] These high-quality AlInN films facilitate the re-examinations of the viewpoints of Naik *et al.*[9] and Grille *et al.*[7] To our surprise, it is found that they are both incorrect.

All AlInN films were grown by MOCVD on C-plane sapphire using an AlN buffer, with pressure around 730 torr and growth temperature around 600 °C. The systematic report on the AlInN growth will be published elsewhere.[13] The Al-contents x are obtained through x-ray diffraction (XRD) measurements employing Vegard's law. Raman spectra are measured on the AlInN surface in a backscattering configuration at room temperature with 514 nm laser excitation.

The Raman spectra of $Al_xIn_{1-x}N$ films are shown in Fig. 1(a). In order to follow the phonon mode evolution, not only indium-rich $Al_xIn_{1-x}N$ ($0.03 \leq x \leq 0.31$) but also some Al-rich $Al_xIn_{1-x}N$ ($0.45 \leq x \leq 0.80$) were prepared and measured by Raman scattering. When $x=0.03$, only the modes at 494.6 cm^{-1} (denoted as e) and 596.0 cm^{-1} (denoted as $a1$) are visible. Since the Al content in this sample is very low, they are easily attributed to E_2^H and $A_1(LO)$ originating from those modes of InN (488 and 586 cm^{-1}, respectively). If Al content increases further, a peak (denoted as $a2$) is developing at the high-frequency side of $a1$ when $x=0.14$. The $a2$

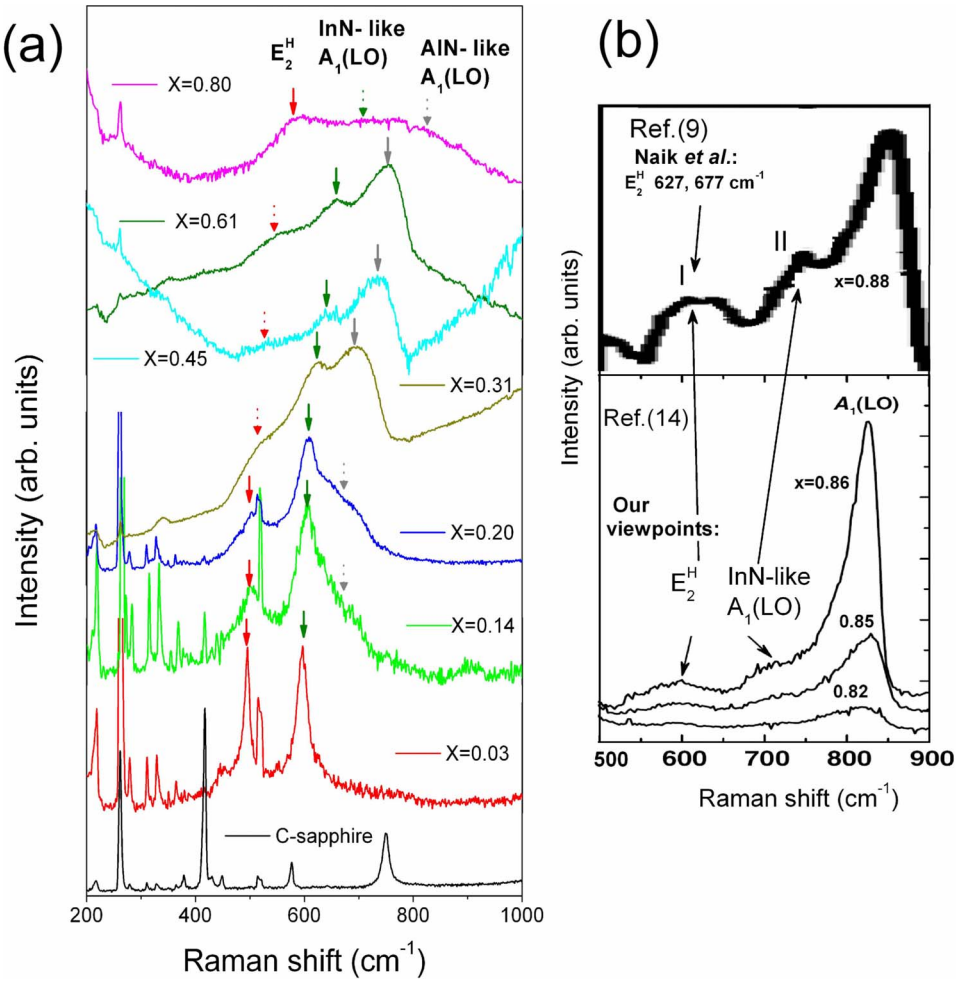

FIG. 1. (Color online) (a) Raman spectra of $Al_xIn_{1-x}N$ films with $0.03 \leq x \leq 0.80$. The spectra at $x=0.45$, 0.61, and 0.80 are given with background subtraction. *C*-plane sapphire Raman spectrum is also given for reference. The phonon frequencies, whose position cannot be determined directly, are deduced by multiple peak fitting and indicated by dotted arrows. (b) The Raman spectra of Al-rich $Al_xIn_{1-x}N$ from Ref. 9 (up side, excitation laser $\lambda=244$ nm) and Ref. 14 (low, excitation laser $\lambda=275.4$ nm). The Al content x are indicated inset; the two maxima in 500–750 cm^{-1} are labeled as I and II, respectively.

mode intensity is enhanced greatly when the Al content x increases. At $x=0.31$, $a2$ mode becomes dominant over $a1$ mode and this dominance is enhanced further for more Al-rich samples. At the same time, with an increase in Al content, $a1$ and $a2$ modes both shift to high frequency. At $x=0.80$, the evolution trend of $a2$ mode to AlN A_1(LO) (890 cm^{-1}) mode can be determined undoubtedly. Therefore we believe that $a2$ mode comes from AlN A_1(LO). The frequency shift and intensity change in $a1$ and $a2$ modes strongly indicate their two-mode behaviors. Therefore we attribute $a1$ mode to InN-like A_1(LO) mode and $a2$ mode to AlN-like A_1(LO) mode.

For e mode, no mode splitting can be detected in Fig. 1(a) within our experimental precision. In addition, the increasing Al content shifts e mode continuously from InN E_2^H (488 cm^{-1}) to AlN E_2^H (657.4 cm^{-1}). We think that these results are due to the one-mode behavior of E_2^H in AlInN and e mode is identified as AlInN E_2^H.

Also in Fig. 1(a), it is noted that the $Al_xIn_{1-x}N$ related Raman signals are badly observed for Al-rich samples, especially when $x=0.8$. As the same as in Ref. 9, this phenomenon can be well understood as resonant excitation effect. According to another recently published $Al_xIn_{1-x}N$ band gap,[12] the excitation laser energy (2.41 eV) used here is near the band gap of $Al_xIn_{1-x}N$ with $x \sim 0.55$. Because the band gap of $Al_{0.8}In_{0.2}N$ sample is much larger than the excitation laser energy, resonant excitation effect is reduced, resulting in the weak AlInN Raman signals. Fortunately, for indium-rich samples, in spite of the factor that the 514 nm photon energy is larger than the sample's band gap, AlInN phonons are still very clear. On the other hand, in Fig. 1(b), Raman spectra of Al-rich AlInN from two other authors,[9,14] whose excitation laser is 244 nm and 275.4 nm, respectively, also show these three phonon maxima clearly and are consistent with our Al-rich samples ($x>0.3$) in line shape. Therefore there is no additional maximum structure produced by 514 nm laser-related resonant excitation effect in Raman spectra of this Brief Report.

These modes' frequencies as functions of Al content for x are extracted and presented in Fig. 2. Additionally, the experimental results provided by Naik *et al.*[9] and the theoretical predictions provided by Grille *et al.*[7] are plotted along

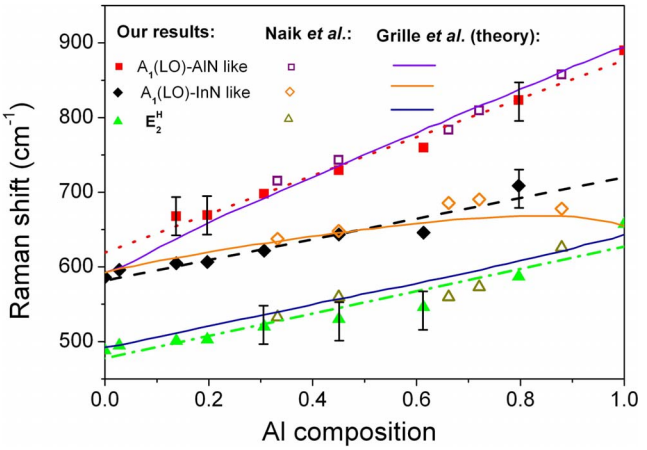

FIG. 2. (Color online) Phonon frequencies versus Al composition x of $Al_xIn_{1-x}N$. The full dots with a bar inside means that their positions are produced indirectly by multiple peak fitting. The dotted and dashed lines are the linear fittings to our experimental data. The data at $x=0,1$ are quoted from Ref. 1. The results of Naik *et al.* in Ref. 9 (in hollow dots) and the theoretical results of Grille *et al.* in Ref. 7 (in full lines) are given for comparison.

with our results in Fig. 2. For our results, the evolution of all three modes can be fitted well by linear functions of x. The major difference between our fitting lines and the theory of Grille *et al.*[7] lies in Al-rich side ($x>0.6$). With respect to Raman shift difference, our line for mode $a1$ is much larger than mode e line but closer to mode $a2$, which support the viewpoint of two-mode A_1(LO). The results of Naik *et al.*[9] agreed well with the predictions of Grille *et al.*[7] when $x>0.6$, especially $x=0.88$, resulting in an obvious deviation from our fitting lines. Figure 1(b) compares their results with the Raman spectra in Ref. 14. We believe that their attributions of twoE_2^H-mode peaks (627 and 677 cm^{-1}) to the maximum I are incorrect [see Fig. 1(b) for the definition of maximum I and II]. The maximum II also changes in Ref. 14 with x value and cannot be overlooked. Therefore the maximum I and II should be attributed to two different mode peaks of AlInN. After removing the unreliable results of Naik *et al.*[9] at $x=0.88$, the experimental points of us and Naik *et al.*[9] can both agree with our fitting lines.

In order to interpret these results semiquantitatively, we resort to the original MREI model proposed by Chang *et al.*[2,5] At the same time, some modifications have to be adopted. In MREI, first, it assumes that the cation and anion of like species vibrate as a rigid unit, i.e., the units vibrate with the same phase and amplitude. Under this assumption, nonpolar mode E_2^H, concerning the two N atoms in one unit cell vibrating in opposite direction, seems to be out of the scope of this MREI model.[8] Therefore our theoretical efforts are limited to only A_1(LO). In the following, LO (TO) means A_1(LO)[A_1(TO)] mode. Second, it assumes the same linear compositional dependence for all force constants involved and all force constants are of the same order in magnitude. We abandon this assumption and set different linear compositional dependence for different force constant. These changes will improve MREI model in interpreting the Raman results of AlInN.

According to MREI model, for $Al_xIn_{1-x}N$, the LO phonon frequency ω_{LO} is determined by the following equation:

$$\begin{vmatrix} -\omega^2 + K_1 + 4\pi Z_1^2/\varepsilon_\infty & K_{12}(\mu_{InN}/\mu_{AlN})^{1/2} + 4\pi Z_1 Z_2/\varepsilon_\infty \\ K_{21}(\mu_{AlN}/\mu_{InN})^{1/2} + 4\pi Z_1 Z_2/\varepsilon_\infty & -\omega^2 + K_2 + 4\pi Z_2^2/\varepsilon_\infty \end{vmatrix} = 0, \tag{1}$$

where

$$K_1 = (1-x)\frac{F_{InN}}{m_N} + \frac{F_{InN}}{m_{In}} + x\frac{F_{InAl}}{m_{In}}, \quad K_2 = x\frac{F_{AlN}}{m_N} + \frac{F_{AlN}}{m_{Al}} + (1-x)\frac{F_{InAl}}{m_{Al}},$$

$$K_{12} = x\frac{F_{AlN}}{m_N} - x\frac{F_{InAl}}{m_{In}}, \quad K_{21} = (1-x)\frac{F_{InN}}{m_N} - (1-x)\frac{F_{InAl}}{m_{Al}}, \tag{2}$$

$$4\pi\frac{Z_1^2}{\varepsilon_\infty} = (\omega_{LO,InN}^2 - \omega_{TO,InN}^2)(1-x), \quad 4\pi\frac{Z_2^2}{\varepsilon_\infty} = (\omega_{LO,AlN}^2 - \omega_{TO,AlN}^2)x,$$

where m_N, m_{In}, m_{Al} are the atomic masses; $\mu_{InN}(\mu_{AlN})$ is the reduced mass of In(Al) and N atoms. F_{AlN} (F_{InN}) is the force constant between Al(In) ion and surrounding N ion. F_{InAl} is the force constant that describes the interaction force between In and Al sublattices. ε_∞ is the high-frequency AlInN dielectric constant and assumed to be varying linearly with Al content x,

$$\varepsilon_\infty = (1-x)\varepsilon_{\infty,InN} + x\varepsilon_{\infty,AlN}. \tag{3}$$

From Eqs. (1) and (2), the boundary conditions for $x=0,1$ are given by

$$\omega_1^2 = \frac{F_{\mathrm{InN},x=0}}{\mu_{\mathrm{InN}}} + \frac{4\pi Z_1^2}{\varepsilon_\infty} = \omega_{\mathrm{LO,InN}}^2$$
$$\omega_2^2 = \frac{F_{\mathrm{AlN},x=0} + F_{\mathrm{InAl},x=0}}{m_{\mathrm{Al}}} = \omega_{a2,x=0}^2,$$
$$\omega_1^2 = \frac{F_{\mathrm{InN},x=1} + F_{\mathrm{InAl},x=1}}{m_{\mathrm{In}}} = \omega_{a1,x=1}^2 \quad (4)$$
$$\omega_2^2 = \frac{F_{\mathrm{AlN},x=1}}{\mu_{\mathrm{AlN}}} + \frac{4\pi Z_2^2}{\varepsilon_\infty} = \omega_{\mathrm{LO,AlN}}^2,$$

where $\omega_{a2,x=0}$ and $\omega_{a1,x=1}$ are determined to be 620 and 720 cm^{-1}, respectively, by extrapolating the ω_{LO} experimental data to $x=0,1$ through the linear fitting functions, as shown in Fig. 2.

The relations between F and TO phonon frequency ω_{LO} are

$$\frac{F_{\mathrm{InN},x=0}}{\mu_{\mathrm{InN}}} = \omega_{\mathrm{TO,InN}}^2, \quad \frac{F_{\mathrm{AlN},x=1}}{\mu_{\mathrm{AlN}}} = \omega_{\mathrm{TO,AlN}}^2. \quad (5)$$

Different from the original MREI method,[2] we assume the linear dependence of the force constant F on Al content x as follows:

$$F_i(x) = F_{i,x=0} + (F_{i,x=1} - F_{i,x=0})x, \quad (i = \mathrm{InN,AlN,InAl}). \quad (6)$$

The values of m_{N}, m_{In}, m_{Al}, μ_{AlN}, and μ_{InN} are well-known, and $\omega_{\mathrm{TO,AlN}}$, $\omega_{\mathrm{LO,AlN}}$, $\omega_{\mathrm{TO,InN}}$, $\omega_{\mathrm{LO,InN}}$, $\varepsilon_{\infty,\mathrm{AlN}}$, and $\varepsilon_{\infty,\mathrm{InN}}$ can be easily found in literature and we take them from Ref. 1. Now only $F_{\mathrm{AlN},x=0}$ and $F_{\mathrm{InN},x=1}$ are unknown and we set them to be adjustable parameters. After the tedious optimization of $F_{\mathrm{AlN},x=0}$ and $F_{\mathrm{InN},x=1}$ on $\omega_{\mathrm{LO,AlInN}}(x)$, we find the optimal values as below

$$F_{\mathrm{InN},x=1} = 1.5F_{\mathrm{InN},x=0} = 3.7424 \times 10^6 \ \mathrm{amu\ cm}^{-2},$$

$$F_{\mathrm{AlN},x=0} = 1.2F_{\mathrm{AlN},x=1} = 4.1311 \times 10^6 \ \mathrm{amu\ cm}^{-2},$$

$$F_{\mathrm{InAl},x=0} = 6.2144 \times 10^6 \ \mathrm{amu\ cm}^{-2},$$

$$F_{\mathrm{InAl},x=1} = 55.772 \times 10^6 \ \mathrm{amu\ cm}^{-2}.$$

According to Chang and Mitra,[2] one-mode behavior for long-wavelength optical phonon in alloy can be realized when the boundary modes $\omega_{a2,x=0}^2 = \frac{F_{\mathrm{AlN},x=0}+F_{\mathrm{InAl},x=0}}{m_{\mathrm{Al}}}$ and $\omega_{a1,x=1}^2 = \frac{F_{\mathrm{InN},x=1}+F_{\mathrm{InAl},x=1}}{m_{\mathrm{In}}}$ are either equal to $\omega_{\mathrm{TO,InN}}^2$ and $\omega_{\mathrm{TO,AlN}}^2$, respectively, or both to zero. As deduced before, compared with F_{InN} and F_{AlN}, the large positive value of F_{InAl}, particularly $F_{\mathrm{InAl},x=1}$, would push the boundary mode frequency well above the values required by one-mode behavior and results in two-mode behavior. We think that this strong positive force interaction between In and Al sublattices is related to the obvious differences between In-N bond and Al-N bond.

One important thing responsible for the bond differences is the factor that InN A_1 reststrahlen band,[2] which means the phonon frequency region from A_1(TO) to A_1(LO) (447–586 cm^{-1}) is so low that it does not overlap with that of AlN (611–890 cm^{-1}). While the GaN A_1 reststrahlen band (531–734 cm^{-1}) overlaps with the AlN A_1 reststrahlen band remarkably. This A_1 reststrahlen band overlap satisfactorily explains why A_1(LO) displays a one-mode behavior in AlGaN but a two-mode behavior in AlInN.

In summary, AlInN over the whole composition range, especially indium-rich AlInN, was prepared and characterized by Raman scattering. The two-mode behavior of A_1(LO) mode is clearly observed for indium-rich AlInN. Through MREI analysis, the force interaction constants among Al, In, and N atoms are deduced. The large positive value of F_{InAl} that describes a strong positive force interaction between In and Al sublattices is believed to be accountable for the two-mode behavior of A_1(LO) modes.

T.-T. Kang thanks H. Terasaki for teaching Raman measurement. This work was supported by the Ministry of Education, Culture, Sports, Science and Technology of Japan through Grant-in-Aid for Scientific Research in Priority Areas (Grant No. 18069005).

*ktt219@163.com

[1] H. Harima, J. Phys.: Condens. Matter **14**, R967 (2002).
[2] I. F. Chang and S. S. Mitra, Phys. Rev. **172**, 924 (1968); Adv. Phys. **20**, 359 (1971).
[3] D. J. Lockwood and Z. R. Wasilewski, Phys. Rev. B **70**, 155202 (2004).
[4] S. Emura, T. Nakagawa, G. Shun-ichi, and S. Shimizu, J. Appl. Phys. **62**, 4632 (1987).
[5] J. Chen and W. Z. Shen, Appl. Phys. Lett. **83**, 2154 (2003).
[6] V. Yu. Davydov, I. N. Goncharuk, A. N. Smirnov, A. E. Nikolaev, W. V. Lundin, A. S. Usikov, A. A. Klochikhin, J. Aderhold, J. Graul, O. Semchinova, and H. Harima, Phys. Rev. B **65**, 125203 (2002) and references therein.
[7] H. Grille, Ch. Schnittler, and F. Bechstedt, Phys. Rev. B **61**, 6091 (2000).
[8] S. G. Yu, K. W. Kim, L. Bergman, M. Dutta, M. A. Stroscio, and J. M. Zavada, Phys. Rev. B **58**, 15283 (1998).
[9] V. M. Naik, W. H. Weber, D. Uy, D. Haddad, R. Naik, Y. V. Danylyuk, M. J. Lukitsch, G. W. Auner, and L. Rimai, Appl. Phys. Lett. **79**, 2019 (2001).
[10] Y. Houchin, A. Hashimoto, and A. Yamamoto, Phys. Status Solidi C **5**, 1571 (2008).
[11] C. Hums, J. Bläsing, A. Dadgar, A. Diez, T. Hempel, J. Christen, A. Krost, K. Lorenz, and E. Alves, Appl. Phys. Lett. **90**, 022105 (2007).
[12] W. Terashima, Song-Bek Che, Y. Ishitani, and A. Yoshikawa, Jpn. J. Appl. Phys., Part 2 **45**, L539 (2006).
[13] Ting-Ting Kang, Akihiro Hashimoto, and Akio Yamamoto, Proceedings of the 69th Autumn Meeting, The Japan Society of Applied Physics, No. 1, 4a-CG-7 (2008).
[14] R. Butté, J.-F. Carlin, E. Feltin, M. Gonschorek, S. Nicolay, G. Christmann, D. Simeonov, A. Castiglia, J. Dorsaz, H. J. Buehlmann, S. Christopoulos, G. Baldassarri, Höger von Högersthal, A. J. D. Grundy, M. Mosca, C. Pinquier, M. A. Py, F. Demangeot, J. Frandon, P. G. Lagoudakis, J. J. Baumberg, and N. Grandjean, J. Phys. D **40**, 6328 (2007).